IRJSE International Research Journal of Science & Engineering
Int. Res. J. of Science & Engineering, Special Issue A12, February, 2023 SJIF Impact Factor 6.70
ISSN: 2322-0015 https://doi.org/10.5281/zenodo.7832368
RESEARCH ARTICLE OPEN ACCESS

Structural and morphological properties of RF sputtered Cu_2ZnSnS_4 thin film for solar cell application

Bansode Anand, Rahane Swati, Jadkar Sandesh R, Chakane Sanjay

Department of Physics, Savitribai Phule Pune University, Pune, 411 007, India
Corresponding author:

Manuscript Details
Available online on https://www.irjse.in
ISSN: 2322-0015

Editor: Dr. Arvind Chavhan

Cite this article as:
Bansode Anand, Rahane Swati, Jadkar Sandesh R, Chakane Sanjay. Structural and morphological properties of RF sputtered Cu_2ZnSnS_4 thin film for solar cell application, *Int. Res. Journal of Science & Engineering,* 2023, Special Issue A12:117-124.
https://doi.org/10.5281/zenodo.7832368

Article published in Special issue of International Conference on "Recent Trends in Materials Science, Synthesis, Characterization and Applications (RTMS-2023)" organized by Department of Physics, Anekant Education Society's, Tuljaram Chaturchand College of Arts, Science and Commerce, Baramati, Dist Pune, Maharashtra, India (Autonomous) date, January 3-4, 2023.

Abstract

We prepared the Kesterite Cu_2ZnSnS_4 (CZTS) absorber thin films deposited by a single target RF magnetron sputtering system. The as-grown CZTS film was sulfurized in an H_2S environment. The structural and optical properties of CZTS thin films were studied by using X-Ray diffraction (XRD), Raman spectrometer, atomic force microscopy (AFM) and UV-Vis spectrophotometer techniques. The XRD analysis showed the presence of a single peak corresponding to the (112) plane. The Raman results confirmed the formation of the pure CZTS phase. The direct optical band gap calculated by Tauc plot analysis is approximately 1.5 eV, which is suitable for solar cell applications. The scanning electron microscopy (SEM) images showed the spherical and uniform morphology of prepared CZTS thin films. We believe that the controlled deposition parameters for the RF sputtering and the generated data presented here will have immediate applications in the deposition of high-quality CZTS-based materials for energy device fabrication.

Keywords: CZTS; Kesterite; RF sputtering; Thin films, CZTS for solar cell; Cu2ZnSnS4.

Introduction

Rapidly vanishing carbon-based fuels resulted in a search for new sources of affordable energy [1]. In the last few decades as well as during the Russia-Ukraine war, some parts of the world faced a shortage of non-renewable energy sources which increased high research demand for renewable energy sources like sunlight or wind energy.

Among the different renewable energy sources, solar energy is economic, efficient, abundant & pollution-free and we get incalculable amounts every second [2].

Due to the highly beneficial solar energy for solar cells, the photovoltaic (PV) industry is booming in current years. It utilizes c-Si and pc-Si as materials for solar cell fabrication. But Si is an indirect band gap material. So, a thick layer of Si is required to act as an absorber layer for higher absorption of the incident solar radiations which results in higher cost of PV devices [2]. In the search for new material which has a direct band gap, researchers have been attracted towards Copper Indium Gallium diselenide (CIGS), Cadmium Telluride (CdTe), and Copper Indium diselenide (CIS). However, the toxicity of Cd & Se interest in CZTS has increased exponentially since this compound is very similar to the well-studied high-efficiency copper indium gallium selenide (CIGS). It has a high absorption coefficient and favourable band gap. CZTS differs from CIGS in that it replaces the indium and gallium with less expensive and earth-abundant zinc and tin, respectively [3]. CZTS is a semiconductor with a direct band gap with values ranging from 1.45-1.6 eV. CZTS mineral is found in nature [4], CZTS exists in form two main structures, namely, stannite type and kesterite type. For the physical deposition of the CZTS layer, many methods like evaporation, pulsed laser deposition (PLD), and sputtering techniques have been used. Sputtering is a satisfactory method for high-volume manufacturing and has benefits like the uniformity of deposited films on a large scale, high deposition rate, and reproducibility of the process [5–8]. Also, sputtering enables interface engineering, tuning of crystallinity, and composition of the films [9–12] & sputtering is a relatively low-cost method to deposit thin films in a vacuum.

Methodology

Preparation of the CZTS thin films

RF Sputtering has many benefits insulators and semiconductors can be sputtered, it has low voltage & pressure, 13.56 MHz ac frequency and it heats up less. CZTS thin films were grown by the single target RF sputtering technique on a bare corning glass substrate. The substrates were pre-cleaned with Acetone and ethanol followed by de-ionized water with sonication and drying in flowing nitrogen (N2) of 99.99% purity. Using rotary and turbo pumps the process sputtering chamber was evacuated to 10^{-6} torr. We used argon gas to maintain an inert atmosphere within the chamber. We used 125-watt RF power for 15 min deposition. The target-to-substrate distance was maintained at 7 cm during deposition time. To ensure uniform deposition, the substrate was rotated at 40 rpm throughout the deposition period.

Result and Discussion

XRD

To study the crystalline structure of synthesized material, an X-ray diffraction analysis is done. The sharp single diffraction peak in the X-Ray Diffraction pattern reflects the single crystalline nature of CZTS nanocrystals. The Peak at 28.40 represents the (112) plane, indicating that the CZTS crystal was successfully formed. The peak well matches with reported data which indicates a tetragonal crystal structure. The observed high intensity and broad shoulder peak located at $2\theta = 28.40$ in all samples reflect the preferential growth of CZTS along the (112) plane. The inter-planar distance of the CZTS nanocrystals for the first-order diffraction is estimated at 3.14 Å, which matches very well with the earlier reported value of 3.12Å [13-15]. The estimated lattice constants for the CZTS kesterite tetragonal structure show concurrence with previously reported values [16].

FWHM and peak intensity (peak height) are used to evaluate the crystallinity. Therefore, the plots of FWHM and peak height of the oriented lattice plane (112) are presented. The average crystallite size is calculated using the Scherrer equation-

$$D_{(hkl)} = k\lambda/\beta \cos\theta$$

where k is the dimensionless shape factor with a value close to unity, λ is the X-ray wavelength, β is the line broadening at half maximum intensity, and θ is the Bragg angle. By this calculation, the average crystallite size estimated is around 5.87 nm. The other important structural parameters like interplanar spacing d_{hkl} and micro strain ϵ_{hkl} are calculated using Bragg's equation $2d\sin\theta = n\lambda$. The various other structural parameters calculated are listed in table 1.

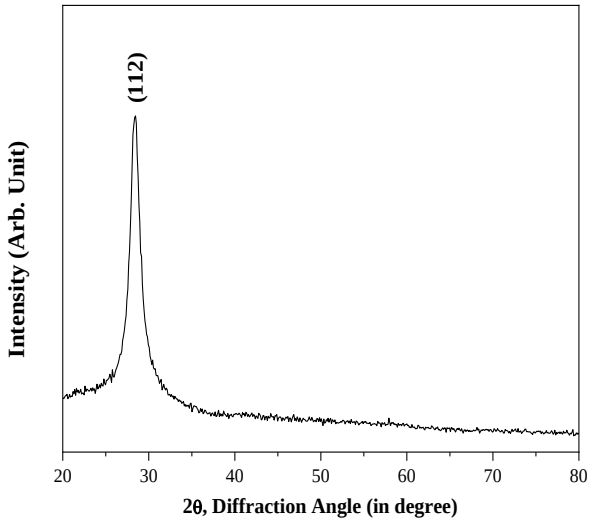

Figure 1. X-ray diffraction pattern for the CZTS nanocrystals indicating excellent crystallinity.

Table 1: Structural parameters, average crystallite size (dx-ray), inter-planar spacing (dhkl), and micro strain for CZTS

2θ	hkl	FWHM (Degree)	FWHM (Rad.)	Average Crystallite size	Dislocation Density $(1/D^2)*10^3$	Microstrain $(\beta/4\tan\theta)*10^{-3}$	d (A^0)
28.40	(112)	1.73	0.0302	5.87 nm	0.04469	24.11	3.14

Raman spectroscopy-

Raman Spectroscopy is useful to characterize the material structure. The phase & purity of the material was confirmed using Raman spectroscopic measurement. The Raman spectrum of CZTS shows the presence of a single peak located at 336 cm^{-1} indicating the absence of any impurity phase. The Raman peak is in accordance with other quaternary chalcogenide semiconductors [17-19]. XRD data and Raman spectra do not show any impurity or secondary phase.

UV-Vis Spectroscopy

The UV-Vis. Spectroscopy measurements were carried out to study the optical properties of CZTS. The UV-Vis. The spectrum of CZTS thin films prepared by RF sputtering is shown in figure 3. The absorption spectrum shows a sharp increase in absorption at about 813 nm. Also, the Tauc plot analysis of this CZTS film is done to calculate the optical band gap. The inset of figure 3 is Tauc plot for CZTS thin films. Absorbance and photon energy are related as,

$(\alpha h\nu)^{1/n} = A*(h\nu - E_g)$,

where A is the proportionality constant, n is an integer and it can be ½ or 2 depending on whether the material is having direct or indirect band gap.

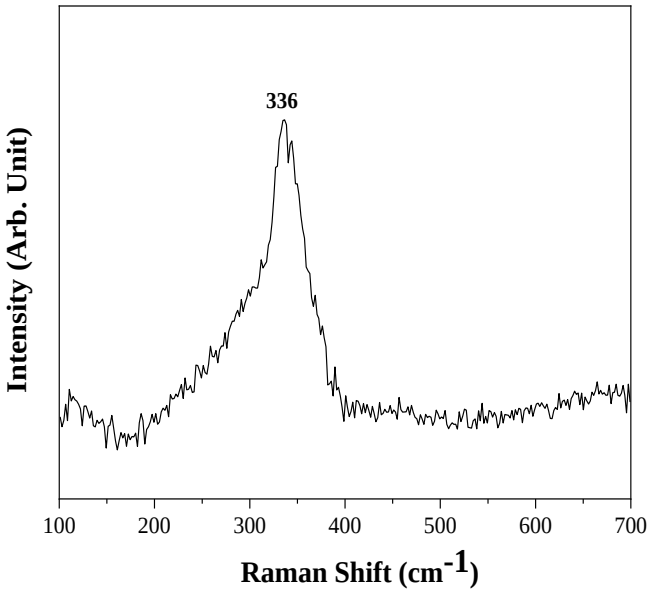

Figure 2. Raman spectrum of CZTS nanocrystals at room temperature.

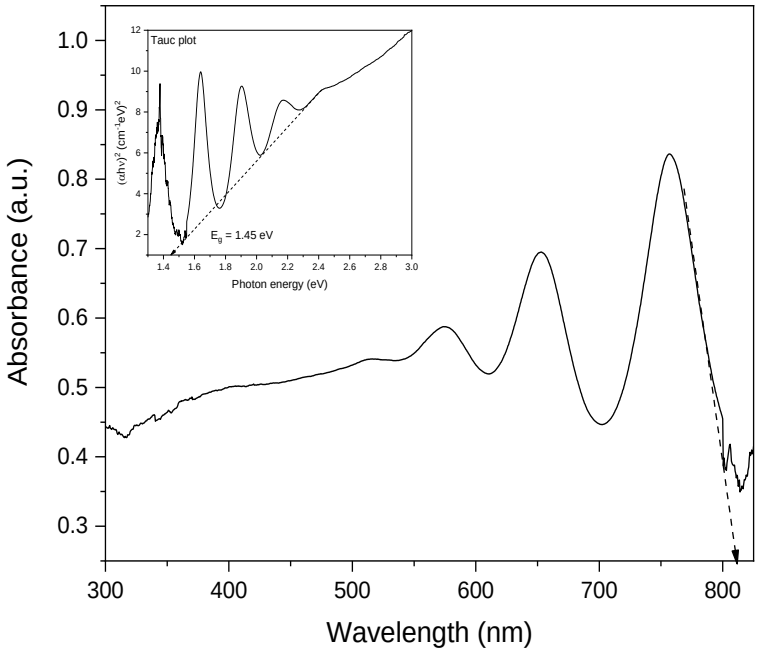

Figure 3. Transmittance of CZTS film (b) Absorption coefficient of the CZTS film, (c) Tauc plot for band gap measurement, (d) Diffuse Reflectance spectra Scanning Electron Microscopy (SEM)

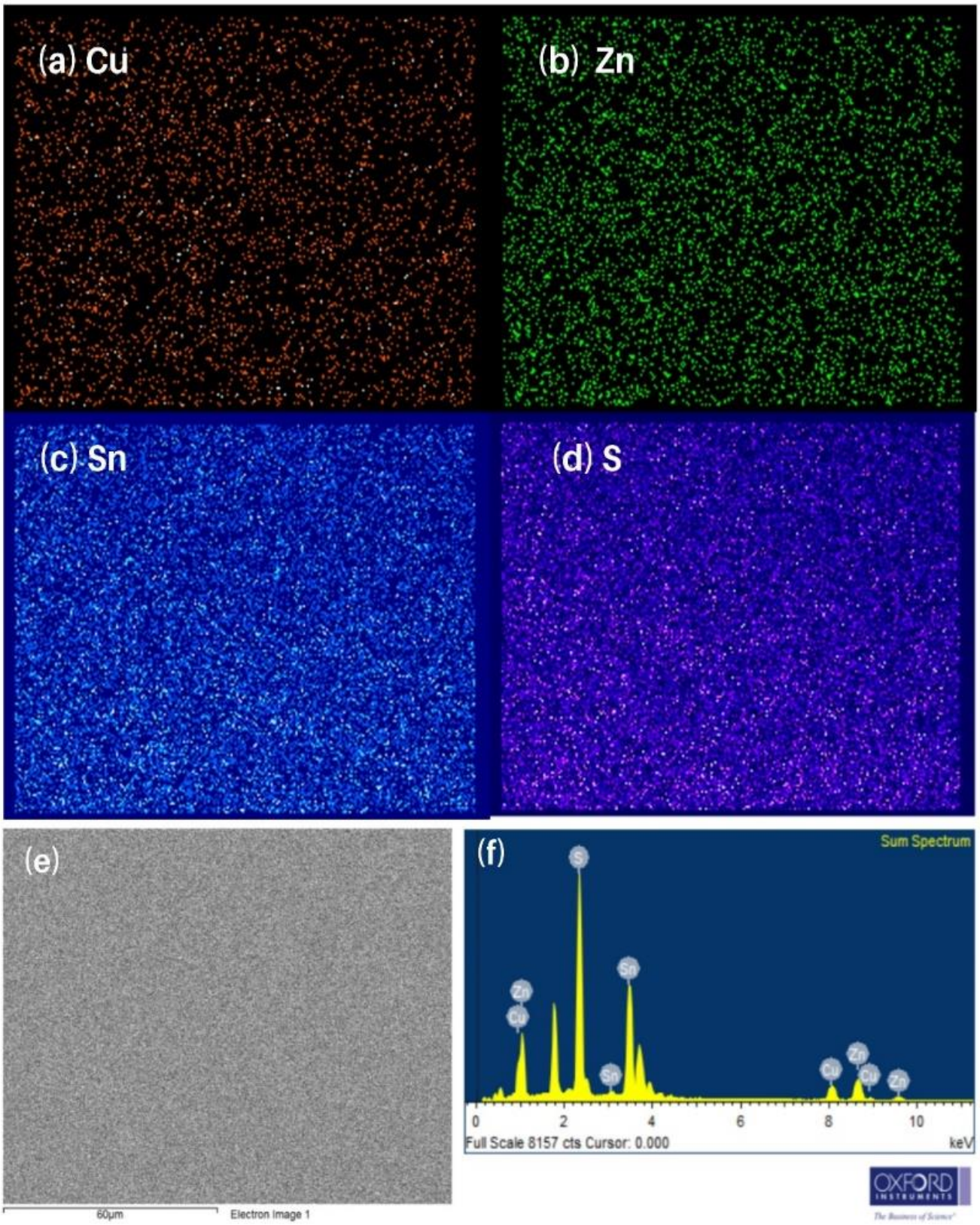

Figure 4: SEM micrograph of CZTS; (a) Cu, (b) Zn (c) Sn, and (d) S.

Table 2: The atomic percentage for metallic elements for CZTS sample using EDS measurements.

Element	Weight %	Atomic %	Ratio
Cu (K)	9.44	8.88	1
Zn (K)	17.05	15.59	1.92
Sn (L)	45.20	22.76	2.56
S (K)	28.30	52.76	5.94

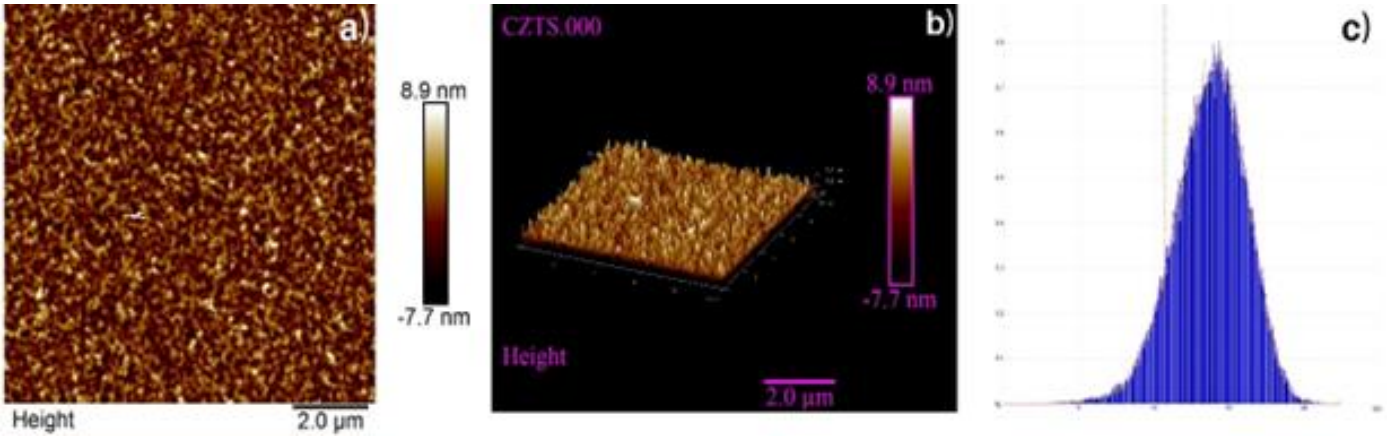

Figure. 5 (a) AFM images of CZTS thin film (b) AFM topographic image of the CZTS thin film (c) Depth Histogram of CZTS height size distributions graph

From Tauc plot analysis, the direct band gap for CZTS film is estimated by extrapolating the linear region of the plot of $(\alpha h\nu)^2$ vs hν and it is found that the estimated band gap is about 1.45 eV. The value estimated is relatively close to the ideal value for photovoltaic solar conversion in the visible region of solar spectrum.

SEM was used to study the morphology of the thin films being deposited. Figure 4 exhibits the micrograph of the as-deposited CZTS thin film which shows grain size with spherical-shaped nanoparticles with uniform distribution. The composition of the films and ratios were analysed by EDS using an S4100 Hitachi with a Rontec EDS system and confirmed with an ICP-MS Thermo X Series.

The atomic percentage and atomic ratios measured by EDS, for the CZTS, are shown in table 1. These compositions are close to the ones reported by Katagiri et al. for their CZTS solar cell with the best efficiency.

Atomic force microscopy (AFM) analysis

Figure 5 shows the surface topography of CZTS films investigated by non-contact atomic force microscopy (NC-AFM). The scan area for all AFM micrographs was 4 μm^2 (2×2 μm^2). AFM micrographs of as-prepared CZTS film revealed textured surface topography. The surface roughness of fabricated CZTS films was evaluated by using AFM. The root means square (rms) surface roughness of the as-prepared CZTS film was found to be 0.30 nm. The most commonly used parameters to calculate surface roughness are the roughness average and the root mean square (RMS) average.

Conclusions

Here, we report the preparation of thin kesterite CZTS films by single target RF magnetron sputtering. The structural, optical, and morphological properties of

prepared films were studied by various characterization methods. The Raman spectra of the samples verified that they were indeed kesterite based on the presence of a large peak at 336 cm−1 indicating no additional impurity phase. The sharp single diffraction peak in the X-Ray Diffraction pattern reflects the single crystalline nature of CZTS nanocrystals. The Peak at 28.40 represents the (112) plane, indicating that the CZTS crystal was successfully formed. AFM analysis revealed that the RMS roughness of the thin films is 0.30 nm. EDS analysis confirmed that the atomic percentage and atomic ratios measured are well matched with the previous reports. UV-Vis spectrum indicated that the direct band gap energies (E_g) of the thin films is 1.45 eV, which is suitable for solar cell applications. Future work in this area will focus on achieving further improvements in CZTS solar absorber quality.

Conflicts of interest: The authors stated that no conflicts of interest.

References

1. M. Jiang and X. Yan, "Solar Cells" InTech, 2013, pp.107-143
2. Kwatra, Priyanka, et al. "Fabrication of CZTS Thin Films based Solar Cells using Vacuum Deposition Techniques: A Status Review." 2019 International Conference on Signal Processing and Communication (ICSC). IEEE, 2019.
3. Dhakal, Tara P., et al. "Characterization of a CZTS thin film solar cell grown by sputtering method." Solar Energy 100 (2014): 23-30.
4. V. A. Tikkiwal, P. Kwatra, S. V. Singh, D. Chandola and H. Gandhoke, "A review on sputter deposited CZTS based thin film solar cells," IEEE International Conference on Computing, Power and Communication Technologies, Galgotia University, G. Noida (UP),2018, pp. 404-408 .
5. G.K. Dalapati, S. Masudy-Panah, S.T. Chua, M. Sharma, T.I. Wong, H.R. Tan, D. Chi, Color tunable low cost transparent heat reflector using copper and titanium oxide for energy saving application, Sci. Rep. 6 (2016) 20182.
6. G.K. Dalapati, S. Masudy-Panah, A. Kumar, C. Cheh Tan, H. Ru Tan, D. Chi, alloyed iron-silicide/silicon solar cells: a simple approach for low cost environmental-friendly photovoltaic technology, Sci. Rep. 5 (2015) 17810.
7. N. Selvakumar, H.C. Barshilia, Review of physical vapor deposited (PVD) spectrally selective coatings for mid- and high-temperature solar thermal applications, Sol. Energy Mater. Sol. Cells 98 (2012) 1–23.
8. N. Selvakumar, A. Biswas, K. Rajaguru, G.M. Gouda, H.C. Barshilia, Nanometer thick tunable AlHfN coating for solar thermal applications: transition from absorber to antireflection coating, Sol. Energy Mater. Sol. Cells 137 (2015) 219–226.
9. S. Masudy-Panah, G.K. Dalapati, K. Radhakrishnan, A. Kumar, H.R. Tan, Reduction of Cu-rich interfacial layer and improvement of bulk CuO property through two-step sputtering for p-CuO/n-Si heterojunction solar cell, J. Appl. Phys. 116 (2014) 74501.
10. S. Masudy-Panah, R. Siavash Moakhar, C.S. Chua, H.R. Tan, T.I. Wong, D. Chi, G.K. Dalapati, Nanocrystal engineering of sputter-grown CuO photocathode for visible-light-driven electrochemical water splitting, ACS Appl. Mater. Interfaces 8 (2016) 1206–1213.
11. S. Masudy-Panah, K. Radhakrishnan, H.R. Tan, R. Yi, T.I. Wong, G.K. Dalapati, Titanium doped cupric oxide for photovoltaic application, Sol. Energy Mater. Sol. Cells 140 (2015) 266–274.
12. S. Masudy-panah, K. Radhakrishnan, T.H. Ru, R. Yi, T.I. Wong, G.K. Dalapati, In situ codoping of a CuO absorber layer with aluminum and titanium: the impact of codoping and interface engineering on the performance of a CuO-based heterojunction solar cell, (n.d.).
13. Tiong, V.T., et al., Phase-selective hydrothermal synthesis of Cu2ZnSnS4 nanocrystals: the effect of the sulphur precursor. CrystEngComm, 2014. 16(20): p. 4306-4313.
14. Xia, D., et al., Characterization of Cu2ZnSnS4 Thin Films Prepared by Solution-based Deposition Techniques. Physics Procedia, 2013. 48: p. 228-234.
15. Lee, S.G., et al., Structural, morphological, compositional, and optical properties of single step electrodeposited Cu2ZnSnS4 (CZTS) thin films for solar cell application. Current Applied Physics, 2014. 14(3): p. 254-258.
16. Bakr, N.A., et al., Deposition and Characterization of Cu2ZnSnS4 Thin Films for Solar Cell Applications International Journal of Applied Engineering Research 2018. 13(6): p. 3379-3388

17. Yan, C.; Huang, C.; Yang, J.; Liu, F.; Liu, J.; Lai, Y.; Li, J.; Liu, Y. Synthesis and characterizations of quaternary Cu2FeSnS4 nanocrystals. Chem. Commun. 2012, 48, 2603−2605.
18. Prabhakar, R. R.; Huu Loc, N.; Kumar, M. H.; Boix, P. P.; Juan, S.; John, R. A.; Batabyal, S. K.; Wong, L. H. Facile water-based spray pyrolysis of earth-abundant Cu2FeSnS4 thin films as an efficient counter electrode in dye-sensitized solar cells. ACS Appl. Mater. Interfaces 2014, 6, 17661−17667.
19. Gillorin, A.; Balocchi, A.; Marie, X.; Dufour, P.; Chane-Ching, J.- Y. Synthesis and optical properties of Cu2CoSnS4 colloidal quantum dots. J. Mater. Chem. 2011, 21, 5615−5619.